THE JOURNAL OF PHYSICAL CHEMISTRY B

Article

pubs.acs.org/JPCB

Self-Templated Free-Radical Polymerization To Form Tactic Chains in Confined Environment

Xinwei Chen,[†,§] Liang Hong,[*,†,‡,§] Chin Yong Lee,[†] Ming En B. Tan,[†,§] Liling Zhang,[†,§] and Jianwen Jiang[†,§]

[†]Department of Chemical and Biomolecular Engineering, National University of Singapore, Singapore 117585, Singapore

[‡]Institute of Materials Research and Engineering, Singapore 117602, Singapore

Supporting Information

ABSTRACT: It is known that the free-radical propagation chain possesses no stereospecificity as the single electron in the p-orbital of radical is equally accessible to the reactants from the bilateral sides, leading to the formation of atactic polymer chains. This sterically uncontrolled radical chain propagation could be rectified through repressing the degrees of freedom of the reactive vinyl monomer molecules by compression as predicted by our molecular simulation. The simulation unveils that molecules undergo ordered alignment upon being compressed to a certain extent to counteract the increase in chemical potential. We validated this concept by polymerizing *N*-isopropylacrylamide, a solid monomer, in a highly confined environment, from which a block copolymers consisting of 68% isotactic blocks was achieved. The additional account was attained from polymerizing liquid styrene under compression, which led to 43.1% isotactic polystyrene blocks. It is thus conceived that an ordered array of vinyl monomers would regulate their steric orientation until they join the propagating polymer chains. In conclusion, specifically, molecular confinement results in self-templated effect and hence offers a unique pathway for stereoselective chain growth.

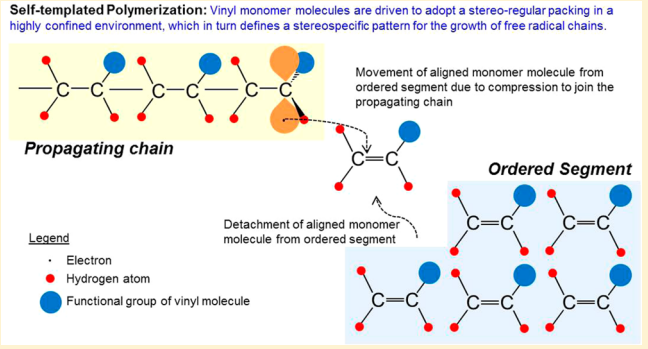

1. INTRODUCTION

The first discovery of stereocontrolled polymerization was accomplished by Ziegler in 1955 and Natta in 1959, which involved the synthesis of isotactic polypropylene.[1] Subsequently, the emergence of chiral metallocene catalysts marked a remarkable progress in the stereospecific polymerization of 1-olefins and has led to the commercialization of isotactic polypropylene—a thermoplastic polymer with a wide range of applications.[1−3] Currently, stereospecific polymers are commonly prepared by ionic or coordination polymerization.[4−7]

Contrary to the ionic and coordination polymerizations, free-radical polymerization has never been a pertinent method for the stereospecific polymerization due to the lack of a necessary asymmetric environment around the planar sp^2-carbon of the free radical chain propagation site. Living radical polymerization methods, such as atom transfer radical polymerization (ATRP)[8,9] and reversible addition−fragmentation chain transfer (RAFT),[10,11] are effective in controlling block copolymers, but have yet to show the capability in affecting the stereochemistry of the polymers. Stereoselective polymerization based on the chain polymerization mechanism has been attempted by using auxiliaries, such as metal triflates, to introduce stereoselectivity into the chain-propagating site.[12,13] Nevertheless, the use of strongly associative metal triflates calls for an addition purification step in the postpolymerization treatment. Recently, stereoregular polymers have been synthesized by utilizing hydrogen bonding rather than coordination to an organotransition metal complex to sterically control the reactive radical sites.[14] Similarly, the postpolymerization removal of the hydrogen-bonding provider from the polymerization system is unavoidable. Nanoporous templates have also been developed to control the tacticity of polymerization,[15] but the effect of nanopores on the stereoregularity of polymerization remains weak due to a lack of the specific asymmetric environment.

In this paper, we explored an alternative strategy relying on highly pressurized environment to conduct stereospecific radical polymerization. The idea originates from the fundamental thermodynamic relation for a closed system: chemical potential of the system escalates when it is subjected to isothermal compression. Acting in response to this change, molecules in the system, such as α,β-conjugated vinyl monomers, will align themselves in a specific manner to resist the rise of chemical potential. Such alignment is energy favorable because it maximizes intermolecular interactions. The computer simulation supports this hypothesis as illustrated in the following sections. Such confined environment would also

Received: April 8, 2013
Revised: May 28, 2013
Published: June 10, 2013

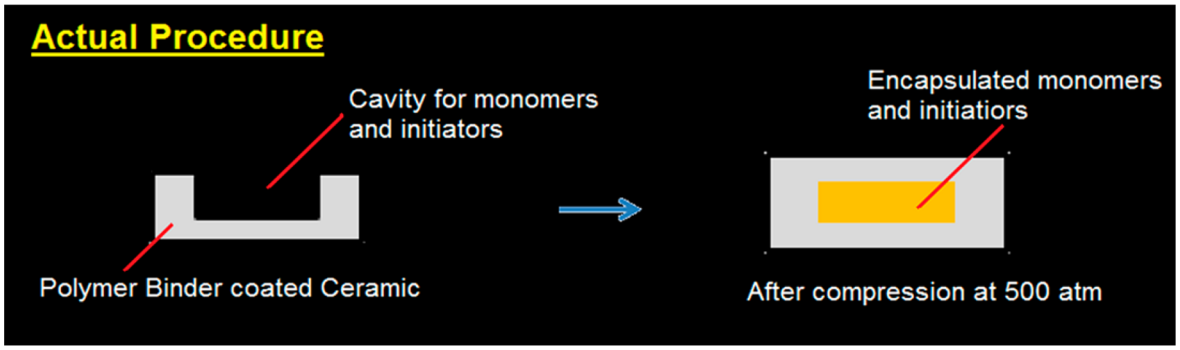

Figure 1. Experimental setup whereby the reacting species are encapsulated in polymer binder coated ceramic particles.

likely to minimize the conformational variety of the generated polymer chains according to a recent study.[16]

Two polymerization systems involving the bulk polymerization in solid and liquid phases were designed to verify if compression can induce stereoregular free-radical polymerization. The solid-phase bulk polymerization was designed by encapsulating *N*-isopropylacrylamide (NIPAM) powder inside a ceramic monolith formed by compression under high pressure.[17−19] Regarding the liquid-phase bulk polymerization, styrene was selected as a vinyl monomer model and the polymerization was conducted in a pressure reactor. Both the simulation and experimental studies suggest that molecular alignment of vinyl monomer form a self-templated environment, in which the monomer molecules undergo stereospecific free-radical-chain growth.

2. EXPERIMENTAL SECTION

2.1. Materials. NIPAM (Aldrich), styrene (≥99%, Aldrich), benzoyl peroxide (BPO, Merck), ammonium persulfate (APS), and iron(II) chloride ($FeCl_2$, Merck) were used as received for the synthesis of polymer. Yttria fully stabilized zirconia (8 mol % Y, YSZ, Stanford Material Corp., USA), poly(vinyl butyral) (PVB, ButvarB79, Solutia, USA), dibutyl phthalate (Acros Organics), sorbitan monostearate (Span-80, Aldrich), and Menhaden fish oil (Sigma Aldrich) were used without further purification for the fabrication of ceramic pellet. Inhibitor remover for removing *tert*-butylcatechol (Aldrich) was used to remove the inhibitor from styrene.

Analytical-grade solvents used for materials processing and characterization include toluene (J.T. Baker, USA), ethyl methyl ketone (MEK, Merck), diethyl ether (Merck), methanol (J.T. Baker), ethanol (Merck), dimethylformamide (DMF, Merck), dimethyl sulfoxide (DMSO, Aldrich), and chloroform (Aldrich). HPLC-grade solvents were used for size exclusion chromatography (SEC) characterization: dimethylformamide (DMF, Merck) and tetrahydrofuran (THF, Tedia, USA). Deuterium-containing solvents were used for nuclear magnetic resonance (NMR) characterization: methyl sulfoxide-d_6 (99.5+ atom % D, Aldrich) and chloroform-*d* (99.8 atom % D, Aldrich).

2.2. Solid-State Polymerization of NIPAM in a Ceramic Capsule. Formulation of binder solution: PVB (2 g) was dissolved in 20 mL of toluene-MEK (v/v = 1). Nonionic surfactant (Span-80, 0.1 g), plasticizer (dibutyl phthalate, 0.1 g) and deflocculating agent (Menhaden fish oil, 0.1 g) were sequentially added to the PVB solution to form a polymer binder solution. Preparation of the binder-coated YSZ powder: YSZ (20 g) with median particle diameter of 0.5−1.0 μm and a specific surface area of 15 m^2/g was blended with the polymer binder solution prepared. The organic solvent was subsequently evaporated, which left the binder-coated YSZ chunks behind. These chunks were then ground and sieved to obtain a fine powder for molding.

Preparation of the initiator−monomer mixture: A given amount of NIPAM was mixed with the initiator couple BPO (0.0535 g)−$FeCl_2$ (0.0439 g) by proportions in weight of 80:1. The monomer−initiator mixture was well mixed by grinding. A given amount of the mixture (0.5 g) was introduced into the cylindrical chamber of a premade YSZ mold, with a diameter of 31 mm. The mixture was then encapsulated in the chamber by covering it with a certain amount of the YSZ powder as shown in Figure 1. The mold was then compressed on a hydraulic press to 500 atm and the pressure was applied for 5 min before the pellet was discharged from the die set. The height of the pellet obtained was about 6 mm.

The prepared YSZ pellet was then transferred to a vacuum oven, which was first vacuumed and then filled with argon as protection atmosphere. The polymerization of the encapsulated NIPAM was carried out at ca. 65 °C under argon for 24 h. The pellet, after this step, was crushed and ground into fine powder. The powder was then dispersed in 20 mL of MEK by stirring for 24 h to dissolve the polymer formed. The resultant suspension was centrifuged at 10 000 rpm for 5 min to separate the organics from the ceramic. The supernatant containing the dissolved organics was gradually introduced into 125 mL of diethyl ether to precipitate PNIPAM and retain the unwanted binder components in the liquid phase. The purified PNIPAM was dried and stored for characterizations. The PNIPAM control sample was synthesized by polymerizing the prior-prepared monomer−initiator mixture only under argon and at 65 °C for 24 h.

2.3. Bulk Polymerization of Styrene in a Pressurized Reactor. To 10 mL of styrene, 0.5 g of BPO was added and the resulting suspension was stirred gently until a homogeneous solution was formed. The solution was then transferred into a stainless steel reactor vessel. The reactor was purged with nitrogen for 5 min before the valve was closed to create an inert atmosphere in the reactor. Nitrogen gas from compressed gas cylinder was then pumped into the reactor to create the required pressure, ranging from 80 to 160 bar. Once the desired pressure was attained, the polymerization was initiated by heating the reactor to 80 °C and allowing to proceed for a day. After reaction, the polymerization vessel was cooled down naturally and the pressure released to atmospheric pressure. Chloroform was added to dissolve the polystyrene (PS) formed. Once a clear solution of PS in chloroform was formed,

dx.doi.org/10.1021/jp403433r | J. Phys. Chem. B 2013, 117, 7826−7832

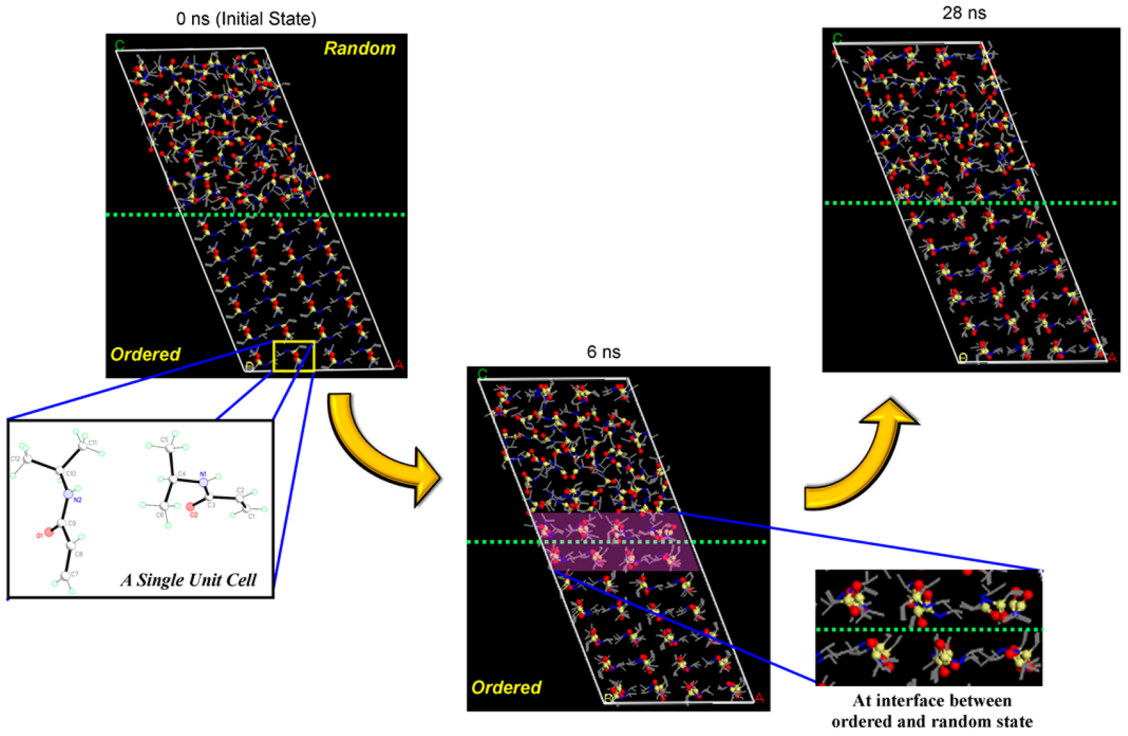

Figure 2. Simulation snapshots of the biphase system at 0, 6, and 28 ns. The green dotted lines indicate the interface between the random and ordered phases. The evolution of the monomers in random phase to ordered manner can be observed with increasing simulation time. (Inset) X-ray structure of a single monoclinic crystal system of NIPAM.

it was poured into an excess of methanol to precipitate PS and to retain unpolymerized styrene in the liquid phase. After filtration and washing with methanol, the purified PS powder was dried at 40 °C and stored.

2.4. Analysis of the Synthesized Polymers. The molecular weights and polydispersity indexes of the synthesized polymers were determined by size exclusion chromatography (SEC) (Waters Styragel gel permeation chromatography) using DMF as the eluent. The synthesized PNIPAM and PS powders were dissolved in HPLC-grade DMF and TMF, respectively, to prepare test samples with the fixed concentration of 1 mg/mL. The samples were then filtered through 0.45 μm PTFE filtration sheet to remove any insoluble residue before analysis. The SEC chromatogram was calibrated by polystyrene standards. Each run lasted for 45 min and 100 μL of sample was injected.

The crystallinities of the synthesized PNIPAM samples were determined on Shimadzu XRD-6000 using Cu target Kα-ray (40 kV and 30 mA) as X-ray source. The scanning range (2θ) covered from 5° to 60° with a scanning speed of 4°/min and 0.02° per step. To map the crystallite and amorphous morphologies of a PNIPAM, a thin film was cast on a carbon-coated copper grid from a dilute acetone solution. The specimen-loaded grid was examined on a transmission electron microscope (TEM) (JEOL JEM-2010). The ^{1}H NMR spectra of the synthesized PNIPAM and PS samples were obtained from an EX-400 spectrometer (JEOL) operated at 400 MHz at room temperature using tetramethylsilane (TMS) (δ = 0.00) as the internal chemical shift standard. To prepare analysis samples, DMSO-d_6 was used to dissolve PNIPAM while chloroform-d_6 to dissolve PS. The concentration of either sample was fixed at ca. 1 mg/mL. It was far more difficult to dissolve PNIPAM synthesized in the pressurized chamber in DMSO-d_6 than to dissolve the control sample; it took approximately 12 h by stirring at 130 °C. The thermal behavior of the PS samples was scrutinized on a Mettler-Toledo differential scanning calorimeter (DSC) with a constant heating/cooling rate of 10 °C/min. The PS samples annealed at 130 °C were compared with the nonannealed counterpart to understand the impact of preparation history on crystallization extent.

2.5. Molecular Dynamics Simulation. As mentioned, the possibility of interfacial self-assembly phenomenon of vinyl monomer under high pressure was first discovered by molecular simulation. This simulation was performed using NIPAM as the monomer. Since the shape and size of NIPAM molecule are essential for the computational model to simulate the actual system, the crystallographic data of NIPAM monomer was determined by single-crystal X-ray diffraction prior to simulation. The analysis revealed that the NIPAM crystal belongs to the $P2/c$ space group with unit cell constants a = 12.8828 Å, b = 12.1712 Å, and c = 9.6280 Å and β = 111.016°. Furthermore, each unit cell consists of two monomers and belongs to the monoclinic system (Figure 2).

To simulate a prepolymerization system, a simulation box that contained 12 (2 × 2 × 3) unit cells with 96 monomers was created. The periodic boundary conditions (PBC) were applied in all three dimensions. Molecular dynamics (MD) simulations were then performed at 343 K and two different pressures (1 and 500 atm). Subsequently, we investigated the ordering of NIPAM monomers at the crystal surface in a biphasic system. As illustrated in Figure 2, the biphasic system consisted of an amorphous phase (randomly distributed unit cells) and a crystal phase (aligned unit cells), each with 96 monomers. The PBC were also exerted in all three dimensions in the biphasic

dx.doi.org/10.1021/jp403433r | J. Phys. Chem. B 2013, 117, 7826−7832

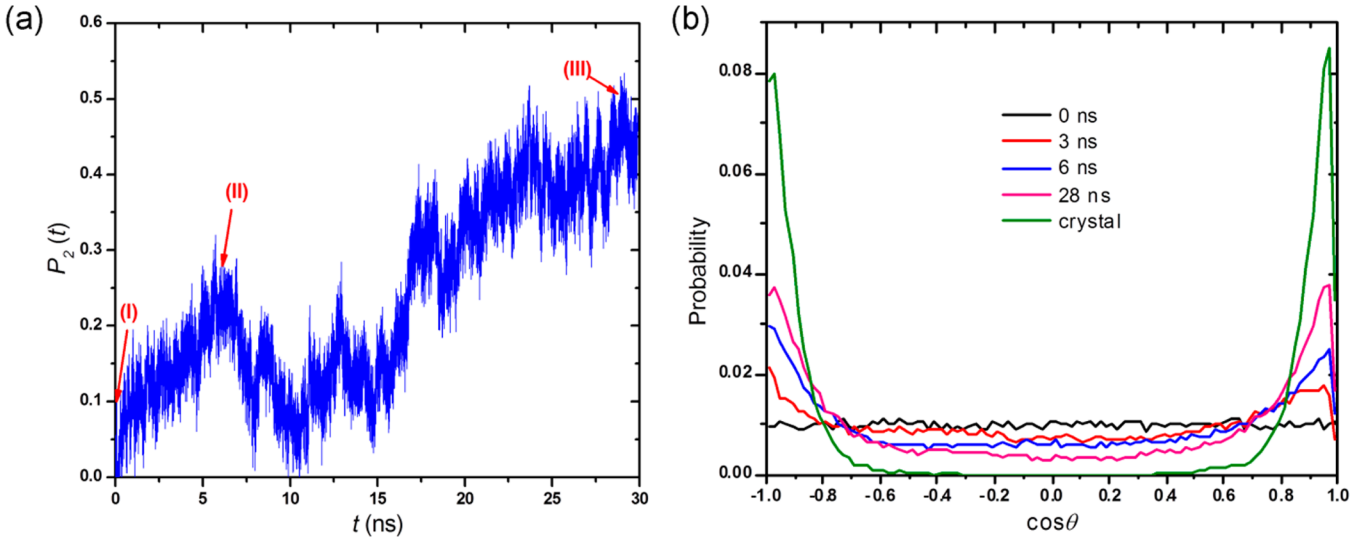

Figure 3. (a) Order parameter in the amorphous phase as a function time. (I), (II), and (III) indicate the simulation duration at 0, 6, and 28 ns. (b) Angle distributions between the C═O bond of NIPAM monomers and the *z*-axis in the amorphous phase at 0, 3, 6, and 28 ns. For comparison, the angle distribution in the crystal phase is also plotted.

system, and a MD simulation was performed at 343 K and 500 atm.

The NIPAM monomers were mimicked by the polymer consistent force field (PCFF),[20−23] which allows the stretching of bonds, bending of bond angles and twisting of dihedral angles. The well depth in the 9−6 potential was rescaled by 1.2 in order to reproduce the experimental crystal density (1.067 g/cm^3). For each system, energy minimization was initially carried out and followed by 30 ns MD simulation. The initial velocities of all atoms were generated from the Maxwell−Boltzmann distribution at the desired temperature. The equations of motion were integrated using the velocity Verlet algorithm with an integration time step of 1 fs. The temperature and pressure were controlled by the Nosé−Hoover thermostat and barostat, respectively, with a time constant of 0.8 ps. All the simulations were performed with package DL_POLY.[24,25]

3. RESULTS AND DISCUSSION

3.1. Confinement Effect in Prepolymerization State by Simulation. The molecular dynamics simulations reveal the propensity that NIPAM molecules adopt orderly array in a confined environment. The molecular state of the monomers in a unit cell was simulated under two different pressures, −1 and 500 atm, and at 343 K. The simulation shows that pressure has a substantial effect on the volume of unit cell, which decreases by 1.6% when the pressure increases from 1 to 500 atm. This contraction implies a decrease in intermonomer distance and that the system moves to a metastable state because of intermolecular repulsion, thereby bringing about the adjustments of molecular orientations.

To investigate the effect of this metastable state on molecular orientation, a biphase system which comprises both ordered and random arrangements of the monoclinic unit cells was constructed (Figure 2). The simulation result shows that ordering of the amorphous phase occurs at the ordered/random interface at the simulated pressure. As shown in Figure 2, the unit cells in the amorphous phase are completely random initially (t = 0 ns). At 6 ns, a distinct layer is formed along the interface with similar molecular orientation to the equivalent monomers in the crystal phase. Subsequently, additional layers with more pronounced ordering are seen at 28 ns. Clearly, this occurrence of ordering is attributed to the specific spatial induction exerted by the monomers in the crystal phase onto those in the amorphous phase.

In a bid to quantify the ordering, we estimated the order parameter $P_2(t) = {}^3/_2\langle\cos^2\theta(t)\rangle - {}^1/_2$ for the amorphous phase, where θ is the angle between the C═O bond of the monomers and the *z*-axis. Despite some fluctuations illustrated in Figure 3a, the order parameter significantly increases with simulation duration. This indicates that the amorphous phase tends to be more ordered in a highly compressed environment. Furthermore, the structural evolution in the amorphous phase was characterized by the distribution of cos θ as a function of simulation duration. Figure 3b shows the angle distributions in the amorphous phase at 0, 3, 6, and 28 ns. Initially, the distribution is isotropic at 0 ns. However, the distribution shifts closer to the one in the crystal phase with increasing simulation duration. This is consistent with the order parameter displayed in Figure 3a. The simulation outcome supports the postulation that the NIPAM unit cells achieve an ordered assembly in a microdomain under confined conditions (500 atm and 343 K). Furthermore, these domains undergo expansion with the extension of time, indicating that the monomer molecules in each domain essentially undergo orderly packing. This provides the basis for tactic polymerization upon initiation by thermal activation.

3.2. Stereoregular Propagation Amid Solid Monomers under Compression. To create a minireactor capable of maintaining the pressure, traditional ceramic pressing method was applied. A given amount of NIPAM monomer was encapsulated inside such reactor and was sealed by isothermal pressing of the binder-coated zirconia pellet at 500 atm. The enclosed NIPAM molecules underwent an ordered array in response to the increase in the chemical potential as predicted by the simulation data. The resultant ordered array was maintained inside the zirconia pellet after the load was removed and throughout the course of polymerization due to the adequately strong binding force of the ceramic polymer binder (PVB) among the zirconia particles.

dx.doi.org/10.1021/jp403433r | J. Phys. Chem. B 2013, 117, 7826−7832

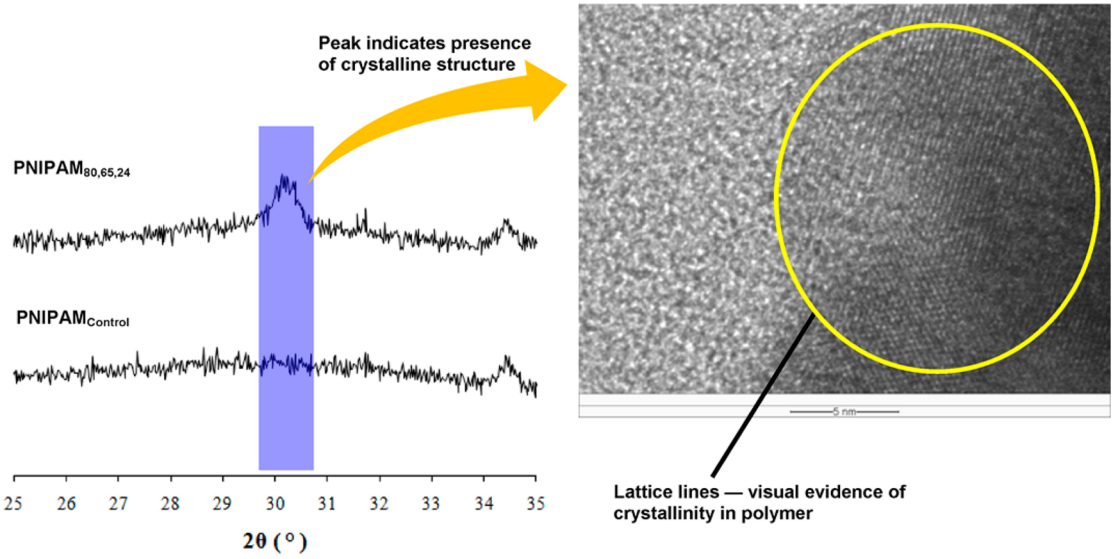

Figure 4. X-ray diffraction spectrum of the isotactic polymer and the control polymer. Crystallinity peak was observed for the isotactic polymer but not for the control polymer. TEM micrograph reflects clearly the crystallinity and amorphous regions of the isotactic polymer.

The resultant PNIPAM exhibited a group of prominent diffraction peaks centered at $2\theta = 30.2°$, indicating the presence of crystallites or small crystal grains that were formed through alignment of tactic chains (Figure 4). Furthermore, the diffuse shape of these peaks suggests that these crystallite domains are surrounded by amorphous boundary layers. This diffraction result is supported by TEM examination (Figure 4): two areas (amorphous and crystalline) can be clearly distinguished in the TEM image. The "grid lines" is indicative of the ordered folding of polymer chains, resulting in the crystalline domains. Its border with the amorphous area is also clearly defined. In contrast, both XRD and TEM do not display the sign for the long-range ordered polymer chain assembly in the control samples prepared by solution polymerization and nonpressured solid-state polymerization, respectively. The latter control sample also eliminates the possibility that zirconia influenced the steric polymerization.

To further determine the tactic chain structure of the PNIPAM synthesized, the ^{1}H NMR spectrum of the polymer in DMSO-d_6 at 25 °C was obtained using an EX-400 spectrometer. The tacticity can be determined on the basis of the relationship between two adjacent monomer units comprising meso (m) and raceme (r) dyads due to the chiral methyne (CH) groups. The ^{1}H peaks of the methylene groups of PNIPAM are expanded (Figure 5) and present two types of dyad: (1) for a meso dyad—the bulky side-chain groups of the two adjacent units are oriented toward the same direction; (2) for a racemic dyad—the two adjacent side-chain groups are oriented toward the opposite directions. The NMR spectrum of the self-templated PNIPAM shows three distinct peaks of which the racemic peak appears between the two meso peaks, a clear indication of predominantly isotactic polymer.[26] The isotactic and syndiotactic degrees can be determined by the area fractions of the meso peaks (m) and of the racemic peak (r), respectively. As such, the polymer is made up of 68% isotactic blocks and 32% syndiotactic blocks in mole. The syndio-block is presumably related to alternating participation of monomers into radical growing chains from adjacent microdomains that are present according to the above section. Regarding the control sample, the meso dyad peak overlaps

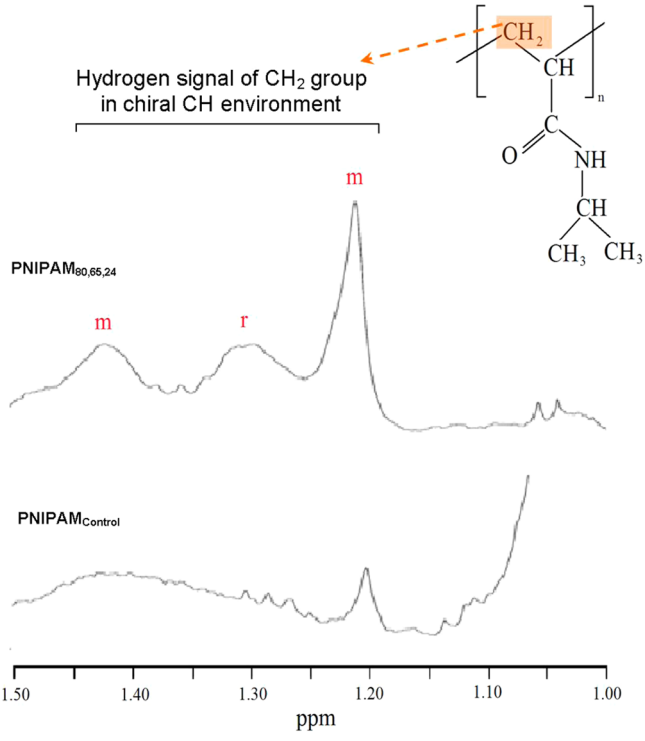

Figure 5. Expanded ^{1}H NMR spectra of main-chain methyne and methylene groups of PNIPAM prepared in DMSO-d_6 at 140 °C.

with the racemic peak due to formation of the atactic chain structure. The degree of isotacticity of the atactic polymer thus cannot be determined.[27] The introduction of stereoregularity into the polymer also makes polymers insoluble in water.[28,29]

3.3. Stereoregular Propagation Amid Liquid Monomers under Compression. With the discovery of pressure-induced stereospecific free-radical polymerization in the solid phase, it is appealing to verify if such phenomenon can be replicated in the liquid phase because the larger intermolecular distance in liquid state increases the difficulty to translate compression to the orientation of monomer molecules. We carried out bulk polymerization of styrene in a pressure reactor,

dx.doi.org/10.1021/jp403433r | J. Phys. Chem. B 2013, 117, 7826−7832

from which the PS sample obtained exhibits a tactic polymer chain configuration against a commercial PS (Figure 6). The

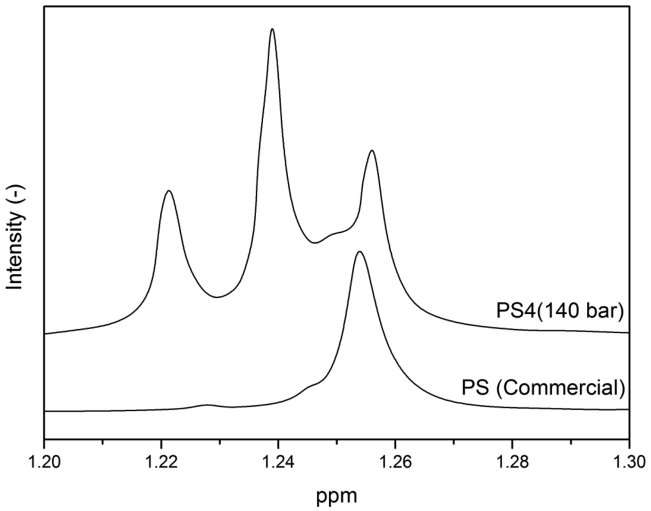

Figure 6. Expanded ^{1}H NMR spectra of main-chain methane and methylene groups of PS prepared in $CHCl_3$-d_6.

methylene proton signal of atactic PS is only a broad resonance, as observed by Bovey et al.[30] Contrary to this, the methylene proton signal of pure isotactic PS exhibits eight peaks as the two methylene protons in isotactic PS are nonequivalent,[31] while the methylene proton signal of syndiotactic PS is only a triplet as the two methylene protons in syndiotactic PS are equivalent.[32] Through the analysis of the chemical shift signals around 1.2−1.3 ppm, the syndiotactic (rr), atactic (mr), and isotactic (mm) triads of methyne carbon hydrogen proton have been calculated with the understanding that rr triad has the lowest chemical shift, followed by mr and then mm. Moreover, the components of these three configuration types, obtained from the ^{1}H NMR analysis, vary with the polymerization pressure used.

Table 1 shows that the triad fractions obtained from the high polymerization pressures ranging from 140 to 160 bar (Table 1) do not fit into either the polymer chain end control model or the enantiomorphic site control model.[33] This is in line with the self-templated polymerization characteristic whereby the ordered packing of vinyl monomers plays the vital role instead of the geometry of chain-propagating site in determining the steric orientation of the side-chain group, e.g., phenyl group in this case. The effect of pressure on the characteristics of triads obtained is clear: in the lower pressure range, the triads are close to the prediction by the polymer chain end control model. Increasing the pressure to 90 bar then yielded a heterotactic triad, which is presumably related to a more chaotic molecular motion accompanying the initial reduction in intermolecular distances. However, it is appealing to note that the stereospecific polymerization of styrene takes place in the pressure range roughly from 140 to 160 bar. We are inclined to consider that the styrene molecules under this compression level take up locally ordered assemblies due to the van der Waals force alignment effect as elucidated above. In addition, the self-templated orderly structure fades away with increasing temperature. Knowing that the tactic polymer chains will lead to the formation of crystallites, we analyzed the calorimetric data of the PS and found that the PS obtained from the pressurized polymerization displays both the latent transition of crystalline phase and the glass transition temperature (T_g) of amorphous phase. Although PS has a characteristic T_g of about 104 °C, the PS samples show a decreasing trend of lower T_g with the increase in the polymerization pressure (Table 1). A rise of the specific latent heat of PS (the area of T_m) was also observed concurrently with the reduction of T_g. This decrease in T_g can be attributed to the shrinkage of amorphous phase in which the interfacial behavior overtook the bulk behavior due to the decrease in chain lengths of the atactic segments. Such deviation of T_g of the interfacial phase from that of the bulk has been observed previously.[34] Nevertheless, the impact of compression on this bulk polymerization system reaches its limit when the pressure was increased to 160 bar at the same temperature. Eventually, the T_g started increasing, indicating the increase in the atactic polymer segment length. Consequently, this increases chain connectivity and hence, segmental motions[35] (i.e., glass transition). This is in line with the NMR analysis as summarized in Table 1. In microscopic scale, when the pressure is raised beyond 160 bar, an individual monomer molecule will become highly dynamic as soon as a neighboring monomer joins a radical chain. This is likely to be the case as the intermolecular repulsions quickly overtake the original metastabilization effect. As a result, the triads generated are similar to those in the lower pressure range, thus moving again toward the chain end control model. Moreover, with the same portion of tactic blocks in a PS chain, the chain length, i.e., molecular weight, affects the degree of crystallinity. A longer polymer chain favors a higher crystallinity due to less perturbation of chain ends. Both increasing temperature and applying too high a pressure brought about a lower molecular weight (Table 1); hence, such condition is detrimental to formation of tactic segments in the polymer chain.

Table 1. Tabulation of Experimental Conditions Employed for the Fabrication of the PS Polymer and the Characteristics of the Synthesized Polymer

			tacticity[a]				
entry	polymerizn press. (bar)	av M_w	mm	mr	rr	characteristics	T_g[b] (°C)
PS1	67.5	32919	10.3	73.1	16.6	atactic	90
PS2	80	24014	14.6	72.4	13.0	atactic	89
PS3	90	20917	0	100	0	atactic	88
PS4	140	15427	31.8	17.2	51.0	isotactic and syndio-rich	79
PS5	160	9267	26.4	30.5	43.1	isotactic and syndio-rich	89
PS6	182	14675	18.3	70.6	11.1	atactic	92

[a]Measured by 400 MHz 1H-NMR spectroscopy. [b]T_g of synthesized polymer after 130 °C for 1 day. Refer to Supporting Information for the DSC graph of the samples.

dx.doi.org/10.1021/jp403433r | J. Phys. Chem. B 2013, 117, 7826−7832

4. CONCLUSION

This study started from the hypothesis that vinyl monomer molecules undergo ordered local assemblies under compression. Molecular simulation by using NIPAM as a molecular model supports the hypothesis. Further experimental validation indicates that local molecule alignment could lead to the self-templated free radical polymerization, giving rise to stereospecific polymer blocks. In the first experimental system, a solid mixture of NIPAM and initiator was encapsulated in an intensely bound ceramic pellet by compression. The polymerization under confined environment yielded a tactic NIPAM copolymer consisting of isotactic and syndiotactic diblocks. This discovery suggests that the orderly arrayed monomer molecules undertake the self-templated polymerization, in which the NIPAM monomer joins growing radical chains with its amide group orienting toward a regular direction. This concept was then extended to the liquid bulk polymerization of styrene under compression. Similarly, the self-templated radical polymerization was replicated when the pressure exceeds 140 bar. The PS chains formed consist of the predominant isotactic and syndiotactic segments. Both NIPAM and styrene have the α,β-conjugated structure, which allows them to take the metastable dipole alignment under compression and undergo stereospecific polymerization in consequence.

■ ASSOCIATED CONTENT

Ⓢ Supporting Information

The glass transition temperatures, T_g, of the PS polymers were determined through the analysis of thermal properties on the DSC graph (Figure S1). This material is available free of charge via the Internet at http://pubs.acs.org.

■ AUTHOR INFORMATION

Corresponding Author

*E-mail: chehongl@nus.edu.sg. Tel.: +65-6516 5029. Fax: +65-6779 1936.

Author Contributions

[§]The manuscript was written through contributions of all authors. All authors have given approval to the final version of the manuscript. These authors contributed equally to the manuscript.

Notes

The authors declare no competing financial interest.

■ ACKNOWLEDGMENTS

The authors express their gratitude to the National Research Foundation of Singapore for funding this research (project title: "Molecular engineering of membrane materials: Research and technology for energy development of hydrogen, natural gas and syngas", WBS: R279-000-261-281).

■ REFERENCES

(1) Moore, E. P. *Polypropylene handbook: polymerization, characterization, properties, processing, applications*; Hanser Publishers: Munich, Germany, 1996.

(2) Marques, M. D. V.; Pombo, C. C.; Silva, R. A.; Conte, A. *Eur. Polym. J.* **2003**, *39* (3), 561−567.

(3) Kaminsky, W. *Macromol. Chem. Phys.* **1996**, *197* (12), 3907−3945.

(4) Chen, E. Y. X. *Chem. Rev.* **2009**, *109* (11), 5157−5214.

(5) Mariott, L. R.; Chen, E. Y. X. *Macromolecules* **2005**, *38* (16), 6822−6832.

(6) Zhang, Y. T.; Ning, Y. L.; Caporaso, L.; Cavallo, L.; Chen, E. Y. X. *J. Am. Chem. Soc.* **2010**, *132* (8), 2695−2709.

(7) Miyake, G. M.; Chen, E. Y. X. *Macromolecules* **2008**, *41* (10), 3405−3416.

(8) Lutz, J. F.; Neugebauer, D.; Matyjaszewski, K. *J. Am. Chem. Soc.* **2003**, *125* (23), 6986−6993.

(9) Lutz, J. F.; Jakubowski, W.; Matyjaszewski, K. *Macromol. Rapid Commun.* **2004**, *25* (3), 486−492.

(10) Hopkins, S.; Carter, S.; MacNeil, S.; Rimmer, S. *J. Mater. Chem.* **2007**, *17* (38), 4022−4027.

(11) Ray, B.; Isobe, Y.; Matsumoto, K.; Habaue, S.; Okamoto, Y.; Kamigaito, M.; Sawamoto, M. *Macromolecules* **2004**, *37* (5), 1702−1710.

(12) Ray, B.; Isobe, Y.; Matsumoto, K.; Habaue, S.; Okamoto, Y.; Kamigaito, M.; Sawamoto, M. *Macromolecules* **2004**, *37* (5), 1702−1710.

(13) Ray, B.; Isobe, Y.; Habaue, S.; Kamigaito, M.; Okamoto, Y. *Polym. J.* **2004**, *36* (9), 728−736.

(14) Hirano, T.; Ishizu, H.; Sato, T. *Polymer* **2008**, *49* (2), 438−445.

(15) Uemura, T.; Ono, Y.; Hijikata, Y.; Kitagawa, S. *J. Am. Chem. Soc.* **2010**, *132* (13), 4917−4924.

(16) Shin, K.; Obukhov, S.; Chen, J. T.; Huh, J.; Hwang, Y.; Mok, S.; Dobriyal, P.; Thiyagarajan, P.; Russell, T. P. *Nat. Mater.* **2007**, *6* (12), 961−965.

(17) Chen, X.; Hong, L.; Tai, X. H. *J. Am. Ceram. Soc.* **2011**, *94* (2), 382−390.

(18) Chen, X. W.; Hong, L. *J. Am. Ceram. Soc.* **2010**, *93* (1), 96−103.

(19) Chen, X. W.; Hong, L.; Phua, J. Y. R. *J. Eur. Ceram. Soc.* **2012**, *32* (14), 3709−3722.

(20) Sun, H. *Macromolecules* **1995**, *28* (3), 701−712.

(21) Sun, H.; Mumby, S. J.; Maple, J. R.; Hagler, A. T. *J. Am. Chem. Soc.* **1994**, *116* (7), 2978−2987.

(22) Sun, H.; Mumby, S. J.; Maple, J. R.; Hagler, A. T. *J. Phys. Chem.* **1995**, *99* (16), 5873−5882.

(23) Sun, H.; Rigby, D. *Spectrochim. Acta, Part A* **1997**, *53* (8), 1301−1323.

(24) Smith, W.; Forester, T. R. *J. Mol. Graphics* **1996**, *14* (3), 136−141.

(25) Smith, W.; Yong, C. W.; Rodger, P. M. *Mol. Simul.* **2002**, *28* (5), 385−471.

(26) Furyk, S.; Zhang, Y. J.; Ortiz-Acosta, D.; Cremer, P. S.; Bergbreiter, D. E. *J. Polym. Sci., Polym. Chem.* **2006**, *44* (4), 1492−1501.

(27) Nuopponen, M.; Kalliomaki, K.; Laukkanen, A.; Hietala, S.; Tenhu, H. *J. Polym. Sci., Polym. Chem.* **2008**, *46* (1), 38−46.

(28) Kitayama, T.; Shibuya, W.; Katsukawa, K. *Polym. J.* **2002**, *34* (5), 405−409.

(29) Ito, M.; Ishizone, T. *J. Polym. Sci., Polym. Chem.* **2006**, *44* (16), 4832−4845.

(30) Bovey, F. A.; Hood, F. P.; Anderson, E. W.; Snyder, L. C. *J. Chem. Phys.* **1965**, *42* (11), 3900−&.

(31) Heatley, F.; Bovey, F. A. *Macromolecules* **1968**, *1* (4), 301−303.

(32) Ishihara, N.; Seimiya, T.; Kuramoto, M.; Uoi, M. *Macromolecules* **1986**, *19* (9), 2464−2465.

(33) Odian, G., *Principles of Polymerization*; Wiley: Hoboken, NJ, 2004.

(34) Zhang, C.; Guo, Y. L.; Priestley, R. D. *Macromolecules* **2011**, *44* (10), 4001−4006.

(35) Kant, R.; Kumar, S. K.; Colby, R. H. *Macromolecules* **2003**, *36* (26), 10087−10094.